Scavenging of reactive dicarbonyls with 2-hydroxybenzylamine reduces atherosclerosis in hypercholesterolemic *Ldlr*$^{-/-}$ mice

Huan Tao[1*], Jiansheng Huang[1*], Patricia G. Yancey[1], John L. Blakemore[1], Youmin Zhang[1], Lei Ding[1], Venkataraman Amarnath[2], John A. Oates[2,3], L. Jackson Roberts II[2], Sean S. Davies[2], MacRae F. Linton[1, 2]

1. Department of Medicine, Division of Cardiovascular Medicine, Atherosclerosis Research Unit, Vanderbilt University School of Medicine, Nashville, TN 37232
2. Department of Pharmacology, Vanderbilt University School of Medicine, Nashville, TN 37232
3. Department of Medicine, Division of Clinical Pharmacology, Vanderbilt University School of Medicine, Nashville, TN 37232

Address correspondence to:
MacRae F. Linton, MD
2220 Pierce Avenue, Nashville, TN
Department of Cardiovascular Medicine, Atherosclerosis Research Unit
Vanderbilt University Medical Center
Email: macrae.linton@vanderbilt.edu

Short title: 2-hydroxybenzylamine attenuates atherosclerosis

*Contributed equally

Abstract

The pathogenesis of atherosclerosis is accelerated by oxidative stress, which produces lipid peroxidation. Among the products of lipid peroxidation are highly reactive dicarbonyls that covalently modify proteins. We investigated the impact of treatment with the dicarbonyl scavenger, 2-hydroxybenzylamine (2-HOBA) on HDL function and atherosclerosis in hyperlipidemic *Ldlr*$^{-/-}$ mice, a model of familial hypercholesterolemia (FH). Compared to mice treated with vehicle, 2-HOBA significantly decreased atherosclerosis in hypercholesterolemic *Ldlr*$^{-/-}$ mice by 31% in the proximal aortas and 60% in *en face* aortas, in the absence of changes in blood lipid levels. 2-HOBA reduced malondialdehyde (MDA) content in HDL, LDL, and in the atherosclerotic lesions. Consuming a Western diet increased plasma MDA-apoAI adduct levels in *Ldlr*$^{-/-}$ mice. 2-HOBA inhibited MDA-apoAI formation and increased the capacity of the mouse HDL to reduce macrophage cholesterol stores. Furthermore, 2-HOBA diminished oxidative stress-induced inflammatory responses in macrophages and reduced the number of TUNEL-positive cells in atherosclerotic lesions by 72%. Importantly, 2-HOBA enhanced efferocytosis and promoted characteristics of stable plaque formation in mice as evidenced by a 69% ($p<0.01$) reduction in necrotic core and by increased collagen content (2.7-fold) and fibrous cap thickness (2.1-fold). HDL from patients with FH had increased MDA content resulting in a reduced ability of FH-HDL to decrease macrophage cholesterol content versus controls. Our results demonstrate that dicarbonyl scavenging with 2-HOBA has multiple atheroprotective effects on lipoproteins and reduces atherosclerosis in a murine model of FH, supporting its potential as a novel therapeutic approach for the prevention and treatment of human atherosclerotic cardiovascular disease.

Key words: 2-hydroxybenzylamine, atherosclerosis, lipoprotein, reactive dicarbonyls, oxidative stress.

Abbreviations:
2-HOBA, 2-hydroxybenzylamine; 4-HOBA, 4-hydroxybenzylamine; MDA, malondialdehyde; 4-HNE, 4-hydroxynonenal; IsoLGs, isolevuglandins; HDL, high-density lipoproteins; LDL, low-density lipoprotein; LDLR, low-density lipoprotein receptor; ApoAI, apolipoprotein AI; ApoB, apolipoprotein B; ROS, reactive oxygen species; IL, interleukin.

Introduction

Atherosclerosis, the underlying cause of heart attack and stroke, is the most common cause of death and disability in the industrial world [1]. Elevated levels of apolipoprotein B (LDL and VLDL) containing lipoproteins and low levels of HDL increase the risk of atherosclerosis [1]. Although lowering LDL with HMG-CoA reductase inhibitors has been shown to reduce the risk of heart attack and stroke in large outcomes trials, substantial residual risk for cardiovascular events remains [2]. Atherosclerosis is a chronic inflammatory disease with oxidative stress playing a critical role [3, 4]. Oxidative modification of apoB containing lipoproteins enhances internalization leading to foam cell formation [1, 5]. In addition, oxidized LDL induces inflammation, immune cell activation, and cellular toxicity [1, 5]. HDL protects against atherosclerosis via multiple roles including promoting cholesterol efflux, preventing LDL oxidation, maintaining endothelial barrier function, and by minimizing cellular oxidative stress and inflammation [1, 4, 6]. HDL-C concentration is inversely associated with cardiovascular disease (CVD) [6], but recent studies suggest that assays of HDL function may provide new independent markers for CVD risk [7, 8]. Evidence has mounted that oxidative modification of HDL compromises its functions, and studies suggest that oxidized HDL is indeed proatherogenic [1, 6, 9].

During lipid peroxidation, highly reactive dicarbonyls, including 4-oxo-nonenal (4-ONE) malondialdehyde (MDA) and isolevuglandins (IsoLGs) are formed. These reactive lipid dicarbonyls covalently bind to DNA, proteins, and phospholipid causing alterations in lipoprotein and cellular functions [1, 10, 11]. In particular, modification with reactive lipid dicarbonyls promotes inflammatory responses and toxicity that may be relevant to atherosclerosis [12, 13, 14, 15]. Identifying effective strategies to assess the contribution of reactive lipid dicarbonyls to disease processes in vivo has been challenging. Although formation of reactive lipid species, including dicarbonyls, theoretically could be suppressed simply by lowering levels of reactive oxygen species (ROS) using dietary antioxidants, the use of antioxidants to prevent atherosclerotic cardiovascular events has proven problematic with most clinical outcomes trials failing to show a benefit [1, 16]. Dietary antioxidants like vitamin C and vitamin E are relatively ineffective suppressors of oxidative injury and lipid peroxidation. In fact, careful studies of patients with hypercholesterolemia found that the doses of vitamin E required to significantly reduce lipid peroxidation were substantially greater than those typically used in most clinical trials [17]. Furthermore, the high doses of antioxidants needed to suppress lipid peroxidation have been associated with significant adverse effects, likely because ROS play critical roles in normal physiology, including protection against bacterial infection and in a number of cell signaling pathways. Finally, for discovery purposes, the use of antioxidants provides little information about the role of reactive lipid dicarbonyls because suppression of ROS inhibits formation of a broad spectrum of oxidatively modified macromolecules besides reactive lipid dicarbonyl species.

An alternative approach to broad suppression of ROS utilizing antioxidants is to use small molecule scavengers that selectively react with lipid dicarbonyl species without altering ROS levels, thereby preventing reactive lipid dicarbonyls from modifying cellular macromolecules without disrupting normal ROS signaling and function. 2-hydroxybenzylamine (2-HOBA) rapidly reacts with lipid dicarbonyls such as IsoLG, ONE, and MDA, but not with lipid monocarbonyls such as 4-hydroxynonenal [15, 18, 19, 20]. The 2-HOBA isomer 4-hydroxybenzylamine (4-HOBA) is ineffective as a dicarbonyl scavenger [21]. Both of these compounds are orally bioavailable, so they can be used to examine the effects of lipid dicarbonyl scavenging in vivo [13, 22]. 2-HOBA protects against oxidative stress associated hypertension [13], oxidant induced cytotoxicity [15],

neurodegeneration, [14] and rapid pacing induced amyloid oligomer formation [23]. While there is evidence that reactive lipid dicarbonyls play a role in atherogenesis [6, 7], to date the effects of scavenging lipid dicarbonyl on the development of atherosclerosis have not been examined.

Here, for the first time, we show that 2-HOBA treatment significantly attenuates atherosclerosis development in hypercholesterolemic *Ldlr*$^{-/-}$ mice. Importantly, 2-HOBA treatment inhibits lesion cell death and necrotic core formation leading to more stable plaque formation as evidenced by increased lesion collagen content and fibrous cap thickness. Consistent with the decrease in atherosclerosis from 2-HOBA treatment being due to scavenging of reactive dicarbonyls, the atherosclerotic lesion MDA content was markedly reduced in 2-HOBA treated versus control mice. We further show that 2-HOBA treatment results in decreased plasma MDA-LDL and MDA-HDL. In addition, MDA-apoAI adduct formation was decreased, and importantly, 2-HOBA treatment caused more efficient HDL function in reducing macrophage cholesterol stores. Thus, scavenging of reactive carbonyls with 2-HOBA has multiple antiatherogenic therapeutic effects that likely contribute to its ability to reduce the development of atherosclerosis in hypercholesterolemic *Ldlr*$^{-/-}$ mice. We also found that HDL from humans with severe familial hypercholesterolemia (FH) contained increased MDA adducts versus control subjects, and that FH-HDL were extremely impaired in reducing macrophage cholesterol stores. Taken together, our studies raise the possibility that reactive dicarbonyl scavenging is a novel therapeutic approach to prevent and treat human atherosclerosis.

Results

2-HOBA treatment attenuates atherosclerosis without altering plasma cholesterol levels in *Ldlr*$^{-/-}$ mice.

Eight week old, female *Ldlr*$^{-/-}$ mice were fed a western diet for 16 weeks and were continuously treated with vehicle alone (water) or water containing either 2-HOBA or 4-HOBA, a nonreactive analogue. Treatment with 2-HOBA reduced the extent of proximal aortic atherosclerosis by 31.1% and 31.5%, compared to treatment with either vehicle or 4-HOBA, respectively (Figures 1A and 1B). In addition, en face analysis of the aorta demonstrated that treatment of female *Ldlr*$^{-/-}$ mice with 2-HOBA reduced the extent of aortic atherosclerosis by 60.3% and 59.1% compared to administration of vehicle and 4-HOBA, respectively (Figures 1C and 1D). Compared to administration of vehicle or 4-HOBA, 2-HOBA treatment did not affect the body weight (Data not shown). In addition, the plasma total cholesterol and triglyceride levels were not significantly different (Figure 1 E) and the lipoprotein distribution was similar between the 3 groups of mice (Supplemental Figure 1) . Consistent with these results, treatment of male *Ldlr*$^{-/-}$ mice with 2-HOBA, under similar conditions of being fed a western diet for 16 weeks, reduced the extent of proximal aortic atherosclerosis by 36%, compared to treatment with water (Supplemental Figure 2A&B) but did not affect the plasma total cholesterol levels (Supplemental Figure 2C). Thus, for the first time, we demonstrate that 2-HOBA treatment significantly decreases atherosclerosis development in an experimental mouse model of FH without changing plasma cholesterol and triglyceride levels. Consistent with the 2-HOBA effects on atherosclerosis being due to reactive lipid dicarbonyl scavenging, the MDA levels in the proximal aorta were reduced by 68.5% and 66.8% in 2-HOBA treated mice compared to mice treated with vehicle alone or 4-HOBA (Figures 2A and 2B).

2-HOBA treatment promotes formation of more stable atherosclerotic plaques in hypercholesterolemic *Ldlr*$^{-/-}$ mice.

As vulnerable plaques exhibit higher risk for acute cardiovascular events [1], we examined the effects of 2-HOBA treatment on characteristics of plaque stabilization by quantitating the

atherosclerotic lesion collagen content, fibrous cap thickness, and necrotic cores (Figures 3A-3D). Compared to administration of vehicle or 4-HOBA, 2-HOBA treatment increased the collagen content of the proximal aorta by 2.7- and 2.6-fold respectively (Figures 3A and 3B). In addition, the fibrous cap thickness was 2.31– and 2.29–fold greater in lesions of 2-HOBA treated mice versus vehicle and 4-HOBA treated mice (Figures 3A and 3C). Importantly, the % of necrotic area in the proximal aorta was decreased by 74.8% and 73.5% in mice treated with 2-HOBA versus vehicle and 4-HOBA (Figures 3A and 3D). Taken together, these data show that 2-HOBA suppresses the characteristics of vulnerable plaque formation in the hypercholesterolemic *Ldlr*$^{-/-}$ mice.

2-HOBA treatment promotes cell survival and efferocytosis and reduces inflammation.
As enhanced cell death and insufficient efferocytosis promote necrotic core formation and destabilization of atherosclerotic plaques, we next examined the effects of 2-HOBA treatment on cell death and efferocytosis in atherosclerotic lesions in the proximal aorta (Figures 4A-4D). Compared to treatment with either vehicle or 4-HOBA, the number of TUNEL positive cells was reduced by 72.9% and 72.4% in the proximal aortic lesions of 2-HOBA treated mice (Figures 4A and 4C). Consistent with reactive lipid dicarbonyl scavenging maintaining efficient efferocytosis, the number of TUNEL positive cells not associated with macrophages was increased by 1.9- and 2.0- fold in lesions of mice treated with vehicle and 4-HOBA versus 2-HOBA (Figures 4B and 4D). In vitro examination of dicarbonyl scavenging with 2-HOBA on the susceptibility of macrophages and endothelial cells to apoptosis in response to H_2O_2 treatment demonstrates that compared to incubation with vehicle or 4-HOBA, 2-HOBA markedly decreased the number of apoptotic cells in both macrophage and endothelial cell cultures (Figures 5A and 5B). In addition, 2-HOBA treatment significantly reduced the macrophage inflammatory response to oxidized LDL as shown by the decreased mRNA levels of IL-1β, IL-6, and TNF-α (Figures 5C-5E). Similar results were observed for the impact of 2-HOBA on the inflammatory cytokine response of macrophages treated with H_2O_2 versus vehicle or 4-HOBA treatment (Figures 5F-5H). Due to the striking impact on inflammatory cyctokines, we measured urinary prostaglandins to evaluate whether 2-HOBA might be inhibiting cyclooxygenase (COX). Urine samples were analyzed for 2,3-dinor-6-keto-PGF1, 11-dehydro TxB2, PGE-M, PGD-M by LC/MS. We found that there were no significant differences in levels of these major urinary prostaglandin metabolites of *Ldlr*$^{-/-}$ mice treated with 2-HOBA compared to the vehicle control (Supplemental Figure 3), indicating that 2-HOBA was not significantly inhibiting COX in vivo in mice. Taken together, these data show that 2-HOBA treatment maintains efficient efferocytosis in vivo and prevents apoptosis and inflammation in response to oxidative stress.

Effects of 2-HOBA on MDA modification and function of lipoproteins and the impact of familial hypercholesterolemia on lipoprotein MDA adduct content and function.
As LDL modification enhances foam cell formation, we examined the effects of in vivo dicarbonyl scavenging on plasma MDA-LDL content (Figure 6A). Compared to treatment with either vehicle or 4-HOBA, the plasma MDA-LDL levels were reduced by 57% and 54% in *Ldlr*$^{-/-}$ mice treated with 2-HOBA (Figure 6A). In addition, dicarbonyl scavenging with 2-HOBA versus vehicle during in vitro modification of LDL with MDA reduced the ability of the LDL to increase cholesterol accumulation in macrophages (Figure 6B). As oxidative modification of HDL impairs its functions, we next examined the effects of 2-HOBA treatment on HDL MDA content and function. Treatment of *Ldlr*$^{-/-}$ mice with 2-HOBA reduced the plasma MDA-HDL levels by 57% and 56% (Figure 7A) compared to treatment with either vehicle or 4-HOBA. Next, we examined ApoAI MDA adduct formation by immunoprecipitating apoAI from plasma and western blotting with an antibody to MDA. After 16 weeks on the western-type diet, *Ldlr*$^{-/-}$ mice treated with vehicle or 4-HOBA had markedly increased plasma levels of MDA-apoAI and reduced plasma apoAI levels compared to *Ldlr*$^{-/-}$ mice consuming a chow diet (Figures 7B and 7C). In contrast,

treatment of *Ldlr*$^{-/-}$ mice consuming a western diet with 2-HOBA dramatically reduced plasma MDA-apoAI adducts and increased apoAI levels (Figures 7B and 7C). Importantly, the HDL isolated from 2-HOBA treated *Ldlr*$^{-/-}$ mice was 2.2- and 1.7-fold more efficient at reducing cholesterol stores in *ApoE*$^{-/-}$ macrophage foam cells versus vehicle and 4-HOBA treated mice (Figure 7D). Consistent with dicarbonyl modification of HDL playing a role in compromising HDL function [24], in vitro modification of HDL with MDA impaired the ability of HDL to reduce the cholesterol content of macrophage foam cells in a dose dependent manner (Figure 7Figure 7E). Importantly, plasma from human subjects with severe FH pre- and post-LDL apheresis (LA) had 5.9-fold and 5.6-fold more MDA-HDL adducts compared to control plasma (Figure 7F). In addition, HDL from FH versus control subjects lacked the ability to reduce the cholesterol content of cholesterol-enriched *ApoE*$^{-/-}$ macrophages (Figure 7G). Taken together, dicarbonyl scavenging with 2-HOBA prevents macrophage foam cell formation by reducing modification of LDL by dicarbonyls and by improving HDL net cholesterol efflux capacity. In addition, our studies suggest that scavenging of reactive lipid dicarbonyls could be a relevant therapeutic approach in humans given that LDL and HDL from subjects with homozygous FH contain increased MDA and enhance foam cell formation.

Discussion

Oxidative stress-induced lipid peroxidation has been implicated in the development of atherosclerosis. Genetic defects and/or environmental factors cause an imbalance between oxidative stress and the ability of the body to counteract or detoxify the harmful effects of oxidation products [1, 3, 25]. The large body of experimental evidence implicating an important role of lipid peroxidation in the pathogenesis of atherosclerosis previously had stimulated interest in the potential for antioxidants to prevent atherosclerotic cardiovascular disease. Although a few trials of dietary antioxidants in humans demonstrated reductions in atherosclerosis and cardiovascular events, the majority of large clinical outcomes trials with antioxidants have failed to show any benefit in terms of reduced cardiovascular events. Possible reasons for the failure of these trials to reduce cardiovascular events, include inadequate doses of antioxidants being used in the trials [1, 16] and the inhibition of normal ROS signaling that may be anti-atherogenic [26]. Treatment with scavengers of reactive dicarbonyl species derived from lipid peroxidation represents a novel alternative therapeutic strategy that will inhibit the adverse effects of ROS without destroying normal signaling mediated by ROS [26]. In the current study, we sought to examine the potential of a reactive lipid dicarbonyl scavenger, to prevent the development of atherosclerosis in *Ldlr*$^{-/-}$ mice. Peroxidation of lipids in tissues/cells or in blood produces a number of highly reactive dicarbonyls that include malondialdehyde, isolevuglandins and 4-oxo-nonenal. These electrophiles can covalently bind to DNA, proteins, and phospholipid causing alterations in lipoprotein and cellular functions [1, 10, 11]. We have recently reported that 2-HOBA can reduce isolevuglandin-mediated HDL modification and dysfunction [27]. Our current studies are the first to examine the effects of dicarbonyl scavenging on atherosclerosis, and we demonstrate that the dicarbonyl scavenger, 2-HOBA, significantly reduces atherosclerosis development in the hypercholesterolemic *Ldlr*$^{-/-}$ mouse model (Figure 1). Importantly, our studies show that 2-HOBA treatment markedly improves features of the stability of the atherosclerotic plaque as evidenced by decreased necrosis and increased fibrous cap thickness and collagen content (Figure 3). Furthermore, dicarbonyl scavenging reduced in vivo MDA modification of HDL, thereby improving its net cholesterol efflux capacity (Figure 7). In addition, MDA modification was increased in HDL from human subjects with familial hypercholesterolemia, which likely contributed to the enhanced foam cell formation induced by FH-HDL (Figure 7). Taken together, dicarbonyl scavenging using 2-HOBA offers therapeutic potential in reducing atherosclerosis development and the risk of clinical events resulting from formation of vulnerable atherosclerotic plaques.

As our studies show that 2-HOBA reduces atherosclerosis development without decreasing plasma cholesterol levels (Figure 1), the atheroprotective effects of 2-HOBA are likely due to scavenging bioactive dicarbonyls. That the effects of 2-HOBA are mediated by their action as dicarbonyl scavengers is further supported by the finding that 4-HOBA, a geometric isomer of 2-HOBA, which is not a scavenger, is not atheroprotective. Prevention of atherosclerosis by removing dicarbonyls substantially strengthens the hypothesis that these dicarbonyls contribute to the pathogenesis of atherogenesis.

HDL mediates a number of atheroprotective functions and evidence has mounted that markers of HDL dysfunction, such as impaired cholesterol efflux capacity, may be a better indicator of CAD risk than HDL-C levels [1, 7, 28, 29, 30]. Patients with FH have previously been shown to have impaired HDL cholesterol efflux capacity, indicative of dysfunctional HDL [31, 32]. Our studies show that consumption of a Western diet by *Ldlr*$^{-/-}$ mice results in enhanced MDA-apoAI adduct formation (Figure 7), and that 2-HOBA treatment dramatically reduces modification of both apoAI and HDL with MDA. Similarly, FH patients had increased plasma levels of MDA-HDL adducts. In addition, in vitro modification of HDL resulted in decreased net cholesterol efflux capacity, which is consistent with studies by Shao and colleagues demonstrating that modification of lipid-free apoAI with MDA blocks ABCA1 mediated cholesterol efflux [24]. Studies have also shown that long term cigarette smoking causes increased MDA-HDL adduct formation, and smoking cessation leads to improved HDL function with increased cholesterol efflux capacity [33]. In line with these results, we found that HDL isolated from 2-HOBA versus vehicle and 4-HOBA treated mice has enhanced capacity to reduce cholesterol stores in macrophage foam cells (Figure 7). Furthermore, HDL from human subjects with familial hypercholesterolemia had markedly increased MDA adducts and severely impaired ability to reduce macrophage cholesterol stores pre- and post-LDL apheresis (Figure 7). Thus, one of the atheroprotective mechanisms of 2-HOBA is likely through preventing formation of dicarbonyl adducts of HDL proteins, thereby preserving HDL net cholesterol efflux function. In addition to decreasing HDL oxidative modification, our studies show that 2-HOBA treatment greatly diminishes the in vivo and in vitro MDA modification of LDL. Studies have shown that MDA modification of LDL promotes foam cell formation and an inflammatory response [34, 35]. Importantly, neutralization of MDA-apoB adducts with antibodies greatly enhances atherosclerosis regression in human apoB100 transgenic *Ldlr*$^{-/-}$ mice [36, 37]. Thus, it is likely that the decreased atherosclerosis with 2-HOBA treatment is also due in part to decreased dicarbonyl modification of apoB.

Evidence has mounted that increased oxidative stress in arterial intima cells is pivotal in inducing ER stress, inflammation, and cell death in atherogenesis [38, 39]. In particular, efficient efferocytosis and limited cell death are critical to preventing the necrosis and the excessive inflammation characteristic of the vulnerable plaque [1, 38, 40]. Our results demonstrate that treatment with 2-HOBA promotes characteristics of more stable atherosclerotic plaques in *Ldlr*$^{-/-}$ mice (Figure 3). Consistent with this possibility, our study shows that 2-HOBA treatment decreased the atherosclerotic lesion MDA adduct content (Figure 2), supporting the ability of dicarbonyl scavenging in the arterial intima to limit oxidative stress induced cell death and destabilization of the plaque. Our studies show that scavenging of dicarbonyls with 2-HOBA in vitro limits oxidative stress induced apoptosis in both endothelial cells and macrophages (Figure 5). The decreased cell death is likely due in part to the greatly diminished inflammatory response to oxidative stress from dicarbonyl scavenging with 2-HOBA, as evidenced by the dramatic reductions in expression of inflammatory cytokines including IL-1β (Figure 5). These results are particularly relevant given the recent results of the CANTOS trial showing that reducing inflammation with canakinumab, an IL-1β neutralizing monoclonal antibody, can

reduce cardiovascular event rates in humans with prior MI and elevated hsCRP [41]. Importantly, treatment with 2-HOBA did not impact levels of urinary prostaglandin metabolites of prostacyclin, thromboxane, PGE2 and PGD2, indicating that 2-HOBA does not result in significant inhibition of cyclooxygenase in mice in vivo (Supplemental Figure 3). Furthermore, 2-HOBA treatment maintained efficient efferocytosis and reduced the number of dead cells in the atherosclerotic lesions (Figure 4). As a result, dicarbonyl scavenging with 2-HOBA promoted formation of features of stable plaques with decreased necrosis and enhanced collagen content and fibrous cap thickness (Figure 3). Hence, the ability of 2-HOBA to limit death and inflammation in arterial cells in response to oxidative stress and to promote efficient efferocytosis in the artery wall provides a novel atheroprotective mechanism whereby dicarbonyl scavenging promotes features of plaque stabilization and reduces atherosclerotic lesion formation.

In conclusion, 2-HOBA treatment suppresses atherosclerosis development in hypercholesterolemic *Ldlr*$^{-/-}$ mice. The atheroprotective effects of 2-HOBA likely result from preventing dicarbonyl adduct formation with plasma apoproteins and intimal cellular components. Treatment with 2-HOBA decreased the formation of MDA-apoAI adducts thereby maintaining efficient HDL function. In addition, the prevention of MDA-apoB adducts decreases foam cell formation and inflammation. Finally, within the atherosclerotic lesion, dicarbonyl scavenging limited cell death, inflammation, and necrosis thereby effectively stabilizing the atherosclerotic plaques. As the atheroprotective effect of 2-HOBA treatment is independent of any action on serum cholesterol levels, 2-HOBA offers real therapeutic potential for decreasing the residual CAD risk that persists in patients treated with HMG-CoA reductase inhibitors.

Materials and Methods

Mice

Ldlr$^{-/-}$ and WT on C57BL/6 background mice were obtained from the Jackson Laboratory. Animal protocols were performed according to the regulations of Vanderbilt University's Institutional Animal Care and Usage Committee. Mice were maintained on chow or a Western-type diet containing 21% milk fat and 0.15% cholesterol (Teklad). Eight week old, female *Ldlr*$^{-/-}$ mice on a chow diet were pretreated with vehicle alone (Water) or containing either 1 g/L of 4-HOBA or 1 g/L of 2-HOBA. After two weeks, the mice continued to receive these treatments but were switched to a Western diet for 16 weeks to induce hypercholesterolemia and atherosclerosis. Similarly, 12 week-old male *Ldlr*$^{-/-}$ mice were pretreated with vehicle alone (water) or containing 3 g/L 2-HOBA for two weeks and were then switched to a Western diet for 16 weeks to induce hypercholesterolemia and atherosclerosis while continuing the treatment with 3 g/L of 2-HOBA or water alone.[42, 43, 44].

Cell Culture

Peritoneal macrophages were isolated from mice 72 hours post injection of 3% thioglycollate and maintained in DMEM plus 10% fetal bovine serum (FBS, Gibco) as previously described [45]. Human aortic endothelial cells (HAECs) were obtained from Lonza and maintained in endothelial cell basal medium-2 plus 1% FBS and essential growth factors (Lonza).

Plasma Lipids and Lipoprotein Distribution Analyses

The mice were fasted for 6 hours, and plasma total cholesterol and triglycerides were measured by enzymatic methods using the reagents from Cliniqa (San-Macros, CA). Fast performance liquid chromatography (FPLC) was performed on an HPLC system model 600 (Waters, Milford, MA) using a Superose 6 column (Pharmacia, Piscataway, NJ).

HDL Isolation from Mouse Plasma and Measurement of HDL Capacity to Reduce Macrophage Cholesterol

HDL was isolated from mouse plasma using HDL Purification Kit (Cell BioLabs, Inc.) following the manufacturer's protocol. Briefly, apoB containing lipoproteins and HDL were sequentially precipitated with dextran sulfate. The HDL was then resuspended and washed. After removing the dextran sulfate, the HDL was dialyzed against PBS. To measure the capacity of the HDL to reduce macrophage cholesterol, apoE$^{-/-}$ macrophages were cholesterol enriched by incubation for 48h in DMEM containing 100 µg protein/ml of acetylated LDL. The cells were then washed, and incubated for 24h in DMEM alone or with 25 µg HDL protein/ml. Cellular cholesterol was measured before and after incubation with HDL using an enzymatic cholesterol assay as described [46].

Human Blood Collection and Measurement of MDA-LDL, MDA-HDL, and MDA-ApoAI

The study was approved by the Vanderbilt University Institutional Review Board (IRB), and all participants gave their written informed consent. The human blood samples from patients with severe FH, who were undergoing LDL apheresis, and healthy controls were obtained using an IRB approved protocol. HDL and LDL were prepared from serum by Lipoprotein Purification Kits (Cell BioLabs, Inc.). Sandwich ELISA was used to measure plasma MDA-LDL and MDA-HDL levels following the manufacturer's instructions (Cell BioLabs, Inc.). Briefly, isolated LDL or HDL samples and MDA-Lipoprotein standards were added onto anti-MDA coated plates, and, after blocking, the samples were incubated with biotinylated anti-apoB or anti-ApoAI primary antibody. The samples were then incubated for 1h with streptavidin-enzyme conjugate and 15 min with substrate solution. After stopping the reaction, the O.D. was measured at 450 nm wavelength. MDA-ApoAI was detected in mouse plasma by immunoprecipitation of ApoAI and western blotting. Briefly, 50 µl of mouse plasma was prepared with 450 µL of IP Lysis Buffer (Pierce) plus 0.5% protease inhibitor mixture (Sigma), and immunoprecipitated with 10 µg of polyclonal antibody against mouse ApoAI (Novus). Then 25 µL of magnetic beads (Invitrogen) was added, and the mixture was incubated for 1h at 4°C with rotation. The magnetic beads were then collected, washed three times, and SDS-PAGE sample buffer with β-mercaptoethanol was added to the beads. After incubation at 70°C for 5 min, a magnetic field was applied to the Magnetic Separation Rack (New England), and the supernatant was used for detecting mouse ApoAI or MDA. For Western blotting, 30-60 µg of proteins was resolved by NuPAGE Bis-Tris electrophoresis (Invitrogen), and transferred onto nitrocellulose membranes (Amersham Bioscience). Membranes were probed with primary rabbit antibodies specific for ApoAI (Novus) or MDA (Cell signaling) and fluorescent tagged IRDye 680 (LI-COR) secondary antibody. Proteins were visualized and quantitated by Odyssey 3.0 Quantification software (LI-COR).

Modification of HDL and LDL with MDA

MDA was prepared immediately before use by rapid acid hydrolysis of maloncarbonyl bis-(dimethylacetal) as described [24]. Briefly, 20 µL of 1 M HCl was added to 200 µL of maloncarbonyl bis-(dimethylacetal), and the mixture was incubated for 45 min at room temperature. The MDA concentration was determined by absorbance at 245 nm, using the coefficient factor 13, 700 M^{-1} cm^{-1}. HDL (10mg of protein /mL) and increasing doses of MDA (0, 0.125 mM, 0.25 mM, 0.5 mM, 1 mM) were incubated at 37 ^{0}C for 24 h in 50 mM sodium phosphate buffer (pH7.4) containing DTPA 100 µM. Reactions were initiated by adding MDA and stopped by dialysis of samples against PBS at 4 ^{0}C. LDL (5 mg/mL) was modified in vitro with MDA (10 mM) in the presence of vehicle alone or with 2-HOBA at 37^{0}C for 24 h in 50 mM sodium phosphate buffer (pH7.4) containing DTPA 100 µM. Reactions were initiated by adding MDA and stopped by dialysis of samples against PBS at 4 ^{0}C. The LDL samples were incubated for 24h with macrophages and the cholesterol content of the cells was measured using an enzymatic cholesterol assay as described [46].

Atherosclerosis Analyses and Cross-section Immunofluorescence Staining
The extent of atherosclerosis was examined both in Oil-Red-O-stained cross-sections of the proximal aorta and by *en face* analysis using the KS300 imaging system (Kontron Elektronik GmbH) [45]. For immunofluorescence staining, 5 µm cross-sections of the proximal aorta were fixed in cold acetone (Sigma), blocked in Background Buster (Innovex), incubated with indicated primary antibodies (MDA and CD68) at 4ºC for overnight. After incubation with fluorescent labeled secondary antibodies at 37C for 1 hour, the nucleus was counterstained with Hoechst. Images were captured with a fluorescence microscope (Olympus IX81) and SlideBook 6 (Intelligent-Image) software and quantitated using ImageJ software (NIH) [47].

In vitro Cellular Apoptosis and Analysis of Lesion Apoptosis and Efferocytosis.
Cell apoptosis was induced as indicated and detected by fluorescent labeled Annexin V staining and quantitated by either Flow Cytometry (BD 5 LSRII) or counting Annexin V positive cells in images captured under a fluorescent microscope. The apoptotic cells in atherosclerotic lesions were measured by TUNEL staining of cross-sections of atherosclerotic proximal aortas as previously described [45]. The TUNEL positive cells not associated with live macrophages were considered free apoptotic cells and macrophage-associated apoptotic cells were considered phagocytosed as a measure of lesion efferocytosis as previously described [45].

Masson's Trichrome Staining
Masson's Trichrome Staining was applied for measurement of atherosclerotic lesion collagen content, fibrous cap thickness and necrotic core size following the manufacture's instructions (Sigma) and as previously described [45]. Briefly, 5 µm cross-sections of proximal atherosclerotic aorta root were fixed with Bouin's solution, stained with hematoxylin for nuclei (black) and biebrich scarlet and phosphotungstic/phosphomolybdic acid for cytoplasm (red), and aniline blue for collagen (blue). Images were captured and analyzed for collagen content, atherosclerotic cap thickness and necrotic core by ImageJ software as described previously [45].

RNA Isolation and Real-Time RT-PCR
Total RNA was extracted and purified using Aurum Total RNA kit (Bio-Rad) according to the manufacturer's protocol. Complementary DNA was synthesized with iScript reverse transcriptase (Bio-Rad). Relative quantitation of the target mRNA was performed using specific primers, SYBR probe (Bio-Rad), and iTaqDNA polymerase (Bio-Rad) on IQ5 Thermocylcer (Bio-Rad) and normalized with 18S, as described earlier. 18S, IL-1β and TNF-α primers used were as described earlier [48].

Liquid chromatography-mass spectrometry analysis of urinary prostaglandin metabolites
Concentrations of PGE-M, tetranor PGD-M, 11-dehydro-TxB^2 (TxB-M) and PGI-M in urine were measured in the Eicosanoid Core Laboratory at Vanderbilt University Medical Center. Urine (1mL) was acidified to pH 3 with HCl. [$^2H_4$]-2,3-dinor-6-keto-PGF1a (internal standard for PGI-M quantification) and [$^2H_4$]-11-dehydro-TxB_2 were added, and the sample was treated with methyloxime HCl to convert analytes to the *O*-methyloxime derivative. The derivatized analytes were extracted using a C-18 Sep-Pak (Waters Corp. Milford, MA USA) and eluted with ethyl acetate as previously described [49]. A [$^2H_6$]-*O*-methyloxime PGE-M deuterated internal standard was then added for PGE-M and PGD-M quantification. The sample was dried under a stream of dry nitrogen at 37°C and then reconstituted in 75 µL mobile phase A for LC/MS analysis.
LC was performed on a 2.0 x 50 mm, 1.7 µm particle Acquity BEH C18 column (Waters Corporation, Milford, MA, USA) using a Waters Acquity UPLC. Mobile phase A was 95:4.9:0.1 (v/v/v) 5 mM ammonium acetate:acetonitrile:acetic acid, and mobile phase B was 10.0:89.9:0.1

(v/v/v) 5 mM ammonium acetate:acetonitrile:acetic acid. Samples were separated by a gradient of 85–5% of mobile phase A over 14 min at a flow rate of 375 μl/min prior to delivery to a SCIEX 6500+ QTrap mass spectrometer.

Urinary creatinine levels are measured using a test kit from Enzo Life Sciences. The urinary metabolite levels in each sample are normalized using the urinary creatinine level of the sample and expressed in ng/mg creatinine.

Statistics

Data are presented as mean ± SEM. The normality of the sample populations was examined by the Kolmogorov-Smirnov test, then differences between mean values were determined by one-way ANOVA (Bonferroni's post-test), Kruskal-Wallis test (Bunn's multiple comparison), Mann-Whitney test, and Student's t-test using GraphPad PRISM. Significance was set for $p < 0.05$.

References

1. M. F. Linton, P. G. Yancey, S. S. Davies, W. G. J. Jerome, E. F. Linton, K. C. Vickers, The Role of Lipids and Lipoproteins in Atherosclerosis. (2000).
2. U. K. Sampson, S. Fazio, M. F. Linton, Residual cardiovascular risk despite optimal LDL cholesterol reduction with statins: the evidence, etiology, and therapeutic challenges. *Curr Atheroscler Rep* **14**, 1-10 (2012).
3. T. J. Anderson, Oxidative stress, endothelial function and coronary atherosclerosis. *Cardiologia* **42**, 701-714 (1997).
4. M. Aviram, Atherosclerosis: cell biology and lipoproteins--inflammation and oxidative stress in atherogenesis: protective role for paraoxonases. *Curr Opin Lipidol* **22**, 243-244 (2011).
5. I. Peluso, G. Morabito, L. Urban, F. Ioannone, M. Serafini, Oxidative stress in atherosclerosis development: the central role of LDL and oxidative burst. *Endocr Metab Immune Disord Drug Targets* **12**, 351-360 (2012).
6. A. Kontush, M. Lindahl, M. Lhomme, L. Calabresi, M. J. Chapman, W. S. Davidson, Structure of HDL: particle subclasses and molecular components. *Handb Exp Pharmacol* **224**, 3-51 (2015).
7. M. Riwanto, L. Rohrer, A. von Eckardstein, U. Landmesser, Dysfunctional HDL: from structure-function-relationships to biomarkers. *Handb Exp Pharmacol* **224**, 337-366 (2015).
8. M. F. Linton, H. Tao, E. F. Linton, P. G. Yancey, SR-BI: A Multifunctional Receptor in Cholesterol Homeostasis and Atherosclerosis. *Trends Endocrinol Metab*, (2017).
9. H. B. Brewer, Jr., D. J. Rader, HDL: structure, function and metabolism. *Prog Lipid Res* **30**, 139-144 (1991).
10. H. Xi, M. Akishita, K. Nagai, W. Yu, H. Hasegawa, M. Eto, K. Kozaki, K. Toba, Potent free radical scavenger, edaravone, suppresses oxidative stress-induced endothelial damage and early atherosclerosis. *Atherosclerosis* **191**, 281-289 (2007).
11. S. Vasdev, V. D. Gill, P. K. Singal, Modulation of oxidative stress-induced changes in hypertension and atherosclerosis by antioxidants. *Exp Clin Cardiol* **11**, 206-216 (2006).
12. L. Guo, Z. Chen, V. Amarnath, P. G. Yancey, B. J. Van Lenten, J. R. Savage, S. Fazio, M. F. Linton, S. S. Davies, Isolevuglandin-type lipid aldehydes induce the inflammatory response of macrophages by modifying phosphatidylethanolamines and activating the receptor for advanced glycation endproducts. *Antioxid Redox Signal* **22**, 1633-1645 (2015).
13. A. Kirabo, V. Fontana, A. P. de Faria, R. Loperena, C. L. Galindo, J. Wu, A. T. Bikineyeva, S. Dikalov, L. Xiao, W. Chen, M. A. Saleh, D. W. Trott, H. A. Itani, A. Vinh, V. Amarnath, K. Amarnath, T. J.

Guzik, K. E. Bernstein, X. Z. Shen, Y. Shyr, S. C. Chen, R. L. Mernaugh, C. L. Laffer, F. Elijovich, S. S. Davies, H. Moreno, M. S. Madhur, J. Roberts, 2nd, D. G. Harrison, DC isoketal-modified proteins activate T cells and promote hypertension. *J Clin Invest* **124**, 4642-4656 (2014).

14. S. S. Davies, C. Bodine, E. Matafonova, B. G. Pantazides, N. Bernoud-Hubac, F. E. Harrison, S. J. Olson, T. J. Montine, V. Amarnath, L. J. Roberts, 2nd, Treatment with a gamma-ketoaldehyde scavenger prevents working memory deficits in hApoE4 mice. *J Alzheimers Dis* **27**, 49-59 (2011).
15. S. S. Davies, E. J. Brantley, P. A. Voziyan, V. Amarnath, I. Zagol-Ikapitte, O. Boutaud, B. G. Hudson, J. A. Oates, L. J. Roberts, 2nd, Pyridoxamine analogues scavenge lipid-derived gamma-ketoaldehydes and protect against H2O2-mediated cytotoxicity. *Biochemistry* **45**, 15756-15767 (2006).
16. J. A. Leopold, Antioxidants and coronary artery disease: from pathophysiology to preventive therapy. *Coron Artery Dis* **26**, 176-183 (2015).
17. L. J. Roberts, 2nd, J. A. Oates, M. F. Linton, S. Fazio, B. P. Meador, M. D. Gross, Y. Shyr, J. D. Morrow, The relationship between dose of vitamin E and suppression of oxidative stress in humans. *Free Radic Biol Med* **43**, 1388-1393 (2007).
18. V. Amarnath, K. Amarnath, K. Amarnath, S. Davies, L. J. Roberts, 2nd, Pyridoxamine: an extremely potent scavenger of 1,4-dicarbonyls. *Chem Res Toxicol* **17**, 410-415 (2004).
19. T. Nakajima, S. S. Davies, E. Matafonova, F. Potet, V. Amarnath, K. A. Tallman, R. A. Serwa, N. A. Porter, J. R. Balser, S. Kupershmidt, L. J. Roberts, 3rd, Selective gamma-ketoaldehyde scavengers protect Nav1.5 from oxidant-induced inactivation. *J Mol Cell Cardiol* **48**, 352-359 (2010).
20. V. Amarnath, K. Amarnath, Scavenging 4-Oxo-2-nonenal. *Chem Res Toxicol* **28**, 1888-1890 (2015).
21. I. Zagol-Ikapitte, V. Amarnath, M. Bala, L. J. Roberts, 2nd, J. A. Oates, O. Boutaud, Characterization of scavengers of gamma-ketoaldehydes that do not inhibit prostaglandin biosynthesis. *Chem Res Toxicol* **23**, 240-250 (2010).
22. I. Zagol-Ikapitte, E. Matafonova, V. Amarnath, C. L. Bodine, O. Boutaud, R. G. Tirona, J. A. Oates, L. J. Roberts Ii, S. S. Davies, Determination of the Pharmacokinetics and Oral Bioavailability of Salicylamine, a Potent gamma-Ketoaldehyde Scavenger, by LC/MS/MS. *Pharmaceutics* **2**, 18-29 (2010).
23. T. N. Sidorova, L. V. Yermalitskaya, L. C. Mace, K. S. Wells, O. Boutaud, J. K. Prinsen, S. S. Davies, L. J. Roberts, 2nd, S. I. Dikalov, C. G. Glabe, V. Amarnath, J. V. Barnett, K. T. Murray, Reactive gamma-ketoaldehydes promote protein misfolding and preamyloid oligomer formation in rapidly-activated atrial cells. *J Mol Cell Cardiol* **79**, 295-302 (2015).
24. B. Shao, S. Pennathur, I. Pagani, M. N. Oda, J. L. Witztum, J. F. Oram, J. W. Heinecke, Modifying apolipoprotein A-I by malondialdehyde, but not by an array of other reactive carbonyls, blocks cholesterol efflux by the ABCA1 pathway. *J Biol Chem* **285**, 18473-18484 (2010).
25. J. C. Calderon, A. Z. Fernandez, A. I. Maria de Jesus, [Atherosclerosis, oxidative stress and physical activity. Review]. *Invest Clin* **49**, 397-410 (2008).
26. S. S. Davies, L. S. Zhang, Reactive Carbonyl Species Scavengers-Novel Therapeutic Approaches for Chronic Diseases. *Curr Pharmacol Rep* **3**, 51-67 (2017).
27. L. S. May-Zhang, V. Yermalitsky, J. Huang, T. Pleasent, M. S. Borja, M. N. Oda, W. G. Jerome, P. G. Yancey, M. F. Linton, S. S. Davies, Modification by isolevuglandins, highly reactive gamma-ketoaldehydes, deleteriously alters high-density lipoprotein structure and function. *J Biol Chem* **293**, 9176-9187 (2018).
28. E. A. Fisher, J. E. Feig, B. Hewing, S. L. Hazen, J. D. Smith, High-density lipoprotein function, dysfunction, and reverse cholesterol transport. *Arterioscler Thromb Vasc Biol* **32**, 2813-2820 (2012).

29. A. Rohatgi, A. Khera, J. D. Berry, E. G. Givens, C. R. Ayers, K. E. Wedin, I. J. Neeland, I. S. Yuhanna, D. R. Rader, J. A. de Lemos, P. W. Shaul, HDL cholesterol efflux capacity and incident cardiovascular events. *N Engl J Med* **371**, 2383-2393 (2014).
30. A. V. Khera, M. Cuchel, M. de la Llera-Moya, A. Rodrigues, M. F. Burke, K. Jafri, B. C. French, J. A. Phillips, M. L. Mucksavage, R. L. Wilensky, E. R. Mohler, G. H. Rothblat, D. J. Rader, Cholesterol efflux capacity, high-density lipoprotein function, and atherosclerosis. *N Engl J Med* **364**, 127-135 (2011).
31. N. Bellanger, A. Orsoni, Z. Julia, N. Fournier, E. Frisdal, E. Duchene, E. Bruckert, A. Carrie, D. Bonnefont-Rousselot, J. Pirault, F. Saint-Charles, M. J. Chapman, P. Lesnik, W. Le Goff, M. Guerin, Atheroprotective reverse cholesterol transport pathway is defective in familial hypercholesterolemia. *Arterioscler Thromb Vasc Biol* **31**, 1675-1681 (2011).
32. M. Ogura, M. Hori, M. Harada-Shiba, Association Between Cholesterol Efflux Capacity and Atherosclerotic Cardiovascular Disease in Patients With Familial Hypercholesterolemia. *Arterioscler Thromb Vasc Biol* **36**, 181-188 (2016).
33. K. Takata, S. Imaizumi, E. Kawachi, Y. Suematsu, T. Shimizu, S. Abe, Y. Matsuo, H. Tsukahara, K. Noda, E. Yahiro, B. Zhang, Y. Uehara, S. Miura, K. Saku, Impact of cigarette smoking cessation on high-density lipoprotein functionality. *Circ J* **78**, 2955-2962 (2014).
34. T. Amaki, T. Suzuki, F. Nakamura, D. Hayashi, Y. Imai, H. Morita, K. Fukino, T. Nojiri, S. Kitano, N. Hibi, T. Yamazaki, R. Nagai, Circulating malondialdehyde modified LDL is a biochemical risk marker for coronary artery disease. *Heart* **90**, 1211-1213 (2004).
35. A. Schiopu, B. Frendeus, B. Jansson, I. Soderberg, I. Ljungcrantz, Z. Araya, P. K. Shah, R. Carlsson, J. Nilsson, G. N. Fredrikson, Recombinant antibodies to an oxidized low-density lipoprotein epitope induce rapid regression of atherosclerosis in apobec-1(-/-)/low-density lipoprotein receptor(-/-) mice. *J Am Coll Cardiol* **50**, 2313-2318 (2007).
36. S. Tsimikas, A. Miyanohara, K. Hartvigsen, E. Merki, P. X. Shaw, M. Y. Chou, J. Pattison, M. Torzewski, J. Sollors, T. Friedmann, N. C. Lai, H. K. Hammond, G. S. Getz, C. A. Reardon, A. C. Li, C. L. Banka, J. L. Witztum, Human oxidation-specific antibodies reduce foam cell formation and atherosclerosis progression. *J Am Coll Cardiol* **58**, 1715-1727 (2011).
37. C. Hjerpe, D. Johansson, A. Hermansson, G. K. Hansson, X. Zhou, Dendritic cells pulsed with malondialdehyde modified low density lipoprotein aggravate atherosclerosis in Apoe(-/-) mice. *Atherosclerosis* **209**, 436-441 (2010).
38. C. M. Scull, I. Tabas, Mechanisms of ER stress-induced apoptosis in atherosclerosis. *Arterioscler Thromb Vasc Biol* **31**, 2792-2797 (2011).
39. D. Bryk, W. Olejarz, D. Zapolska-Downar, The role of oxidative stress and NADPH oxidase in the pathogenesis of atherosclerosis. *Postepy Hig Med Dosw (Online)* **71**, 57-68 (2017).
40. I. Tabas, Apoptosis and efferocytosis in mouse models of atherosclerosis. *Curr Drug Targets* **8**, 1288-1296 (2007).
41. P. M. Ridker, B. M. Everett, T. Thuren, J. G. MacFadyen, W. H. Chang, C. Ballantyne, F. Fonseca, J. Nicolau, W. Koenig, S. D. Anker, J. J. P. Kastelein, J. H. Cornel, P. Pais, D. Pella, J. Genest, R. Cifkova, A. Lorenzatti, T. Forster, Z. Kobalava, L. Vida-Simiti, M. Flather, H. Shimokawa, H. Ogawa, M. Dellborg, P. R. F. Rossi, R. P. T. Troquay, P. Libby, R. J. Glynn, Antiinflammatory Therapy with Canakinumab for Atherosclerotic Disease. *N Engl J Med* **377**, 1119-1131 (2017).
42. P. A. VanderLaan, C. A. Reardon, R. A. Thisted, G. S. Getz, VLDL best predicts aortic root atherosclerosis in LDL receptor deficient mice. *J Lipid Res* **50**, 376-385 (2009).
43. L. Song, C. Leung, C. Schindler, Lymphocytes are important in early atherosclerosis. *J Clin Invest* **108**, 251-259 (2001).
44. D. D. Smith, X. Tan, O. Tawfik, G. Milne, D. J. Stechschulte, K. N. Dileepan, Increased aortic atherosclerotic plaque development in female apolipoprotein E-null mice is associated with

elevated thromboxane A2 and decreased prostacyclin production. *J Physiol Pharmacol* **61**, 309-316 (2010).
45. H. Tao, P. G. Yancey, V. R. Babaev, J. L. Blakemore, Y. Zhang, L. Ding, S. Fazio, M. F. Linton, Macrophage SR-BI mediates efferocytosis via Src/PI3K/Rac1 signaling and reduces atherosclerotic lesion necrosis. *J Lipid Res* **56**, 1449-1460 (2015).
46. P. Robinet, Z. Wang, S. L. Hazen, J. D. Smith, A simple and sensitive enzymatic method for cholesterol quantification in macrophages and foam cells. *J Lipid Res* **51**, 3364-3369 (2010).
47. S. M. Hartig, Basic image analysis and manipulation in ImageJ. *Curr Protoc Mol Biol* **Chapter 14**, Unit14 15 (2013).
48. K. J. Livak, T. D. Schmittgen, Analysis of relative gene expression data using real-time quantitative PCR and the 2(-Delta Delta C(T)) Method. *Methods* **25**, 402-408 (2001).
49. A. Mohebati, G. L. Milne, X. K. Zhou, A. J. Duffield-Lillico, J. O. Boyle, A. Knutson, B. P. Bosworth, P. J. Kingsley, L. J. Marnett, P. H. Brown, E. G. Akpa, E. Szabo, A. J. Dannenberg, Effect of zileuton and celecoxib on urinary LTE4 and PGE-M levels in smokers. *Cancer Prev Res (Phila)* **6**, 646-655 (2013).

Acknowledgments and Sources of Funding

The analyses of urinary prostaglandin metabolites were performed in the Vanderbilt University Eicosanoid Core Laboratory. This work was supported by National Institutes of Health Grants: HL116263 and DK59637 (Lipid, Lipoprotein and Atherosclerosis Core of the Vanderbilt MouseMetabolic Phenotype Centers).

Disclosures

Drs. Linton, Davies, Amarnath, Oates, and Roberts are inventors on a patent application for the use of 2-HOBA and related dicarbonyl scavengers for the treatment of cardiovascular disease. All the other authors declare no financial conflicts of interest.

Authors' contribution

H.T. designed and performed key experiments, acquired and analyzed data, wrote manuscript; J.H. designed and performed parts of experiments, acquired and analyzed data; P.G.Y. designed research, analyzed data, wrote manuscript; J. L. B. and Y.Z. and L.D. conducted parts of the experiments; V.A. , J.A.O. , L.J.R.II, S.S.D.. analyzed data and modified manuscript; K M. F. L. designed research, analyzed data, wrote manuscript.

Huan Tao and Jiansheng Huang made equal contribution

Figure 1

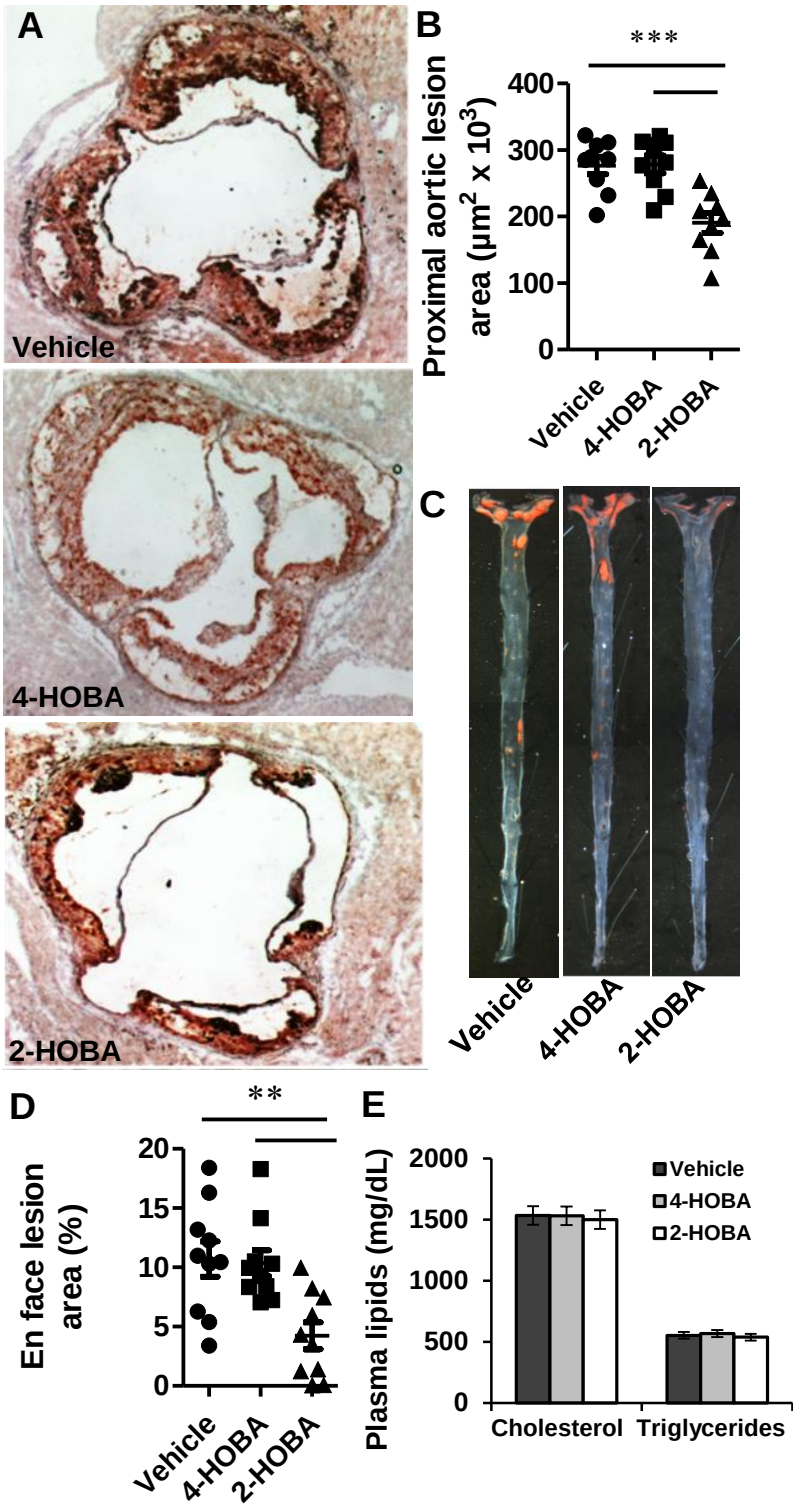
A
Vehicle
4-HOBA
2-HOBA
B
***
Proximal aortic lesion area (μm² x 10³)
400
300
200
100
0
Vehicle
4-HOBA
2-HOBA
C
Vehicle
4-HOBA
2-HOBA
D
**
En face lesion area (%)
20
15
10
5
0
Vehicle
4-HOBA
2-HOBA
E
Plasma lipids (mg/dL)
2000
1500
1000
500
0
Vehicle
4-HOBA
2-HOBA
Cholesterol
Triglycerides

Figure 1. 2-HOBA attenuates atherosclerosis in the hypercholesterolemic female *Ldlr*$^{-/-}$ mice. 8-week *Ldlr*$^{-/-}$ female mice were pretreated with 1 g/L 2-HOBA or 1 g/L 4-HOBA (nonreactive analogue) or vehicle (water) for 2 weeks and then the treatment was continued for 16 weeks during which the mice were fed a Western diet. (A and C) Representative images show Red-Oil-O stain in proximal aorta root sections (A) and in open-pinned aortas (C). (B and D) Quantitation of the mean Oil-Red-O stainable lesion area in aorta root sections (B) and en face aortas (D). N = 9 or 10 per group, ** $p<0.01$, *** $p<0.001$. (E) The plasma total cholesterol and triglyceride levels (F). N = 9 or 10 per group.

Figure 2

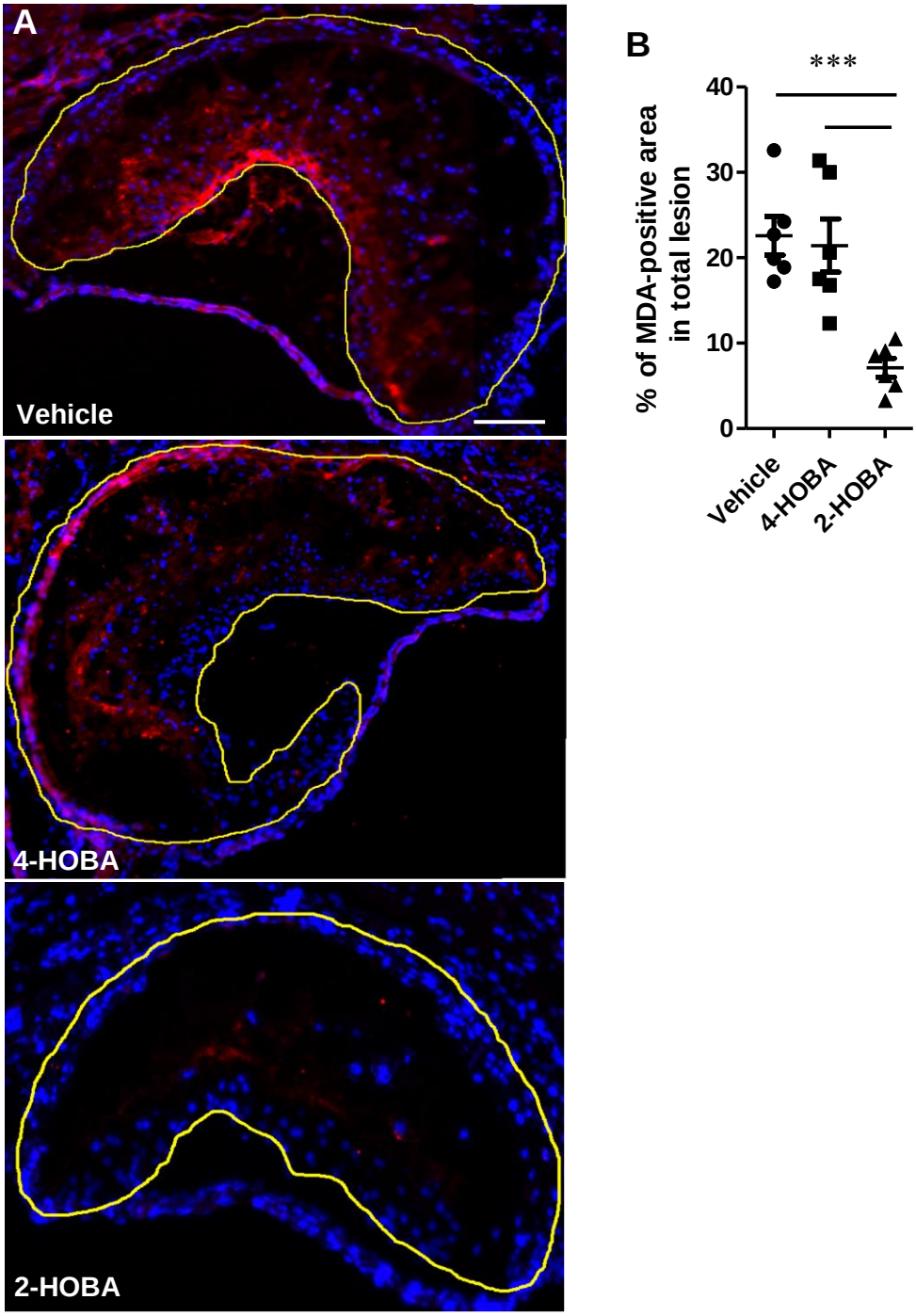

Figure 2. 2-HOBA decreases the MDA content of proximal aortic atherosclerotic lesions in *Ldlr*$^{-/-}$ mice. MDA was detected by immunofluorescence using anti-MDA primary antibody and fluorescent-labeled secondary antibody. Nuclei were counterstained with Hoechst (Blue). (A) Representative images show MDA staining (Red) in proximal aortic root sections. (B) Quantitation of the mean MDA positive lesion area in aortic root sections using ImageJ software. Data are presented as mean ± SEM, N = 6 per group, *** $p<0.001$.

Figure 3

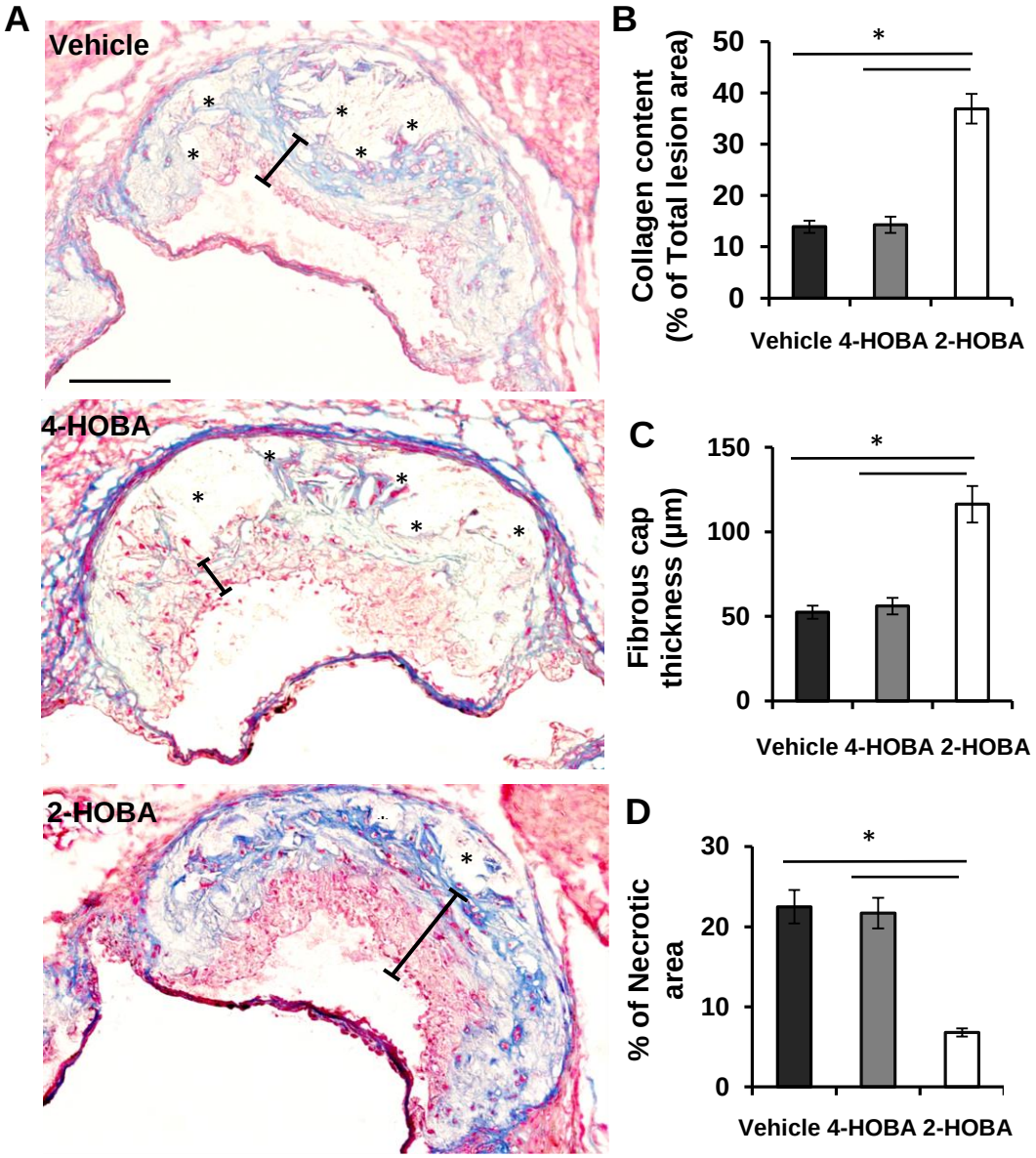

Figure 3. 2-HOBA promotes stable atherosclerotic plaque formation in *Ldlr*$^{-/-}$ mice. Masson's Trichrome stain was applied to analyze atherosclerotic lesion stability in proximal aorta sections of *Ldlr*$^{-/-}$ mice. (A) Representative images show Masson's Trichrome stain in aorta root sections. The collagen content (B), fibrous cap thickness (C), and necrotic area (D) were quantitated using ImageJ software. N = 8 per group. * $p < 0.05$, scale bar = 100 µm. Blue shows collagen, Red, cytoplasm, Black, nuclei.

Figure 4

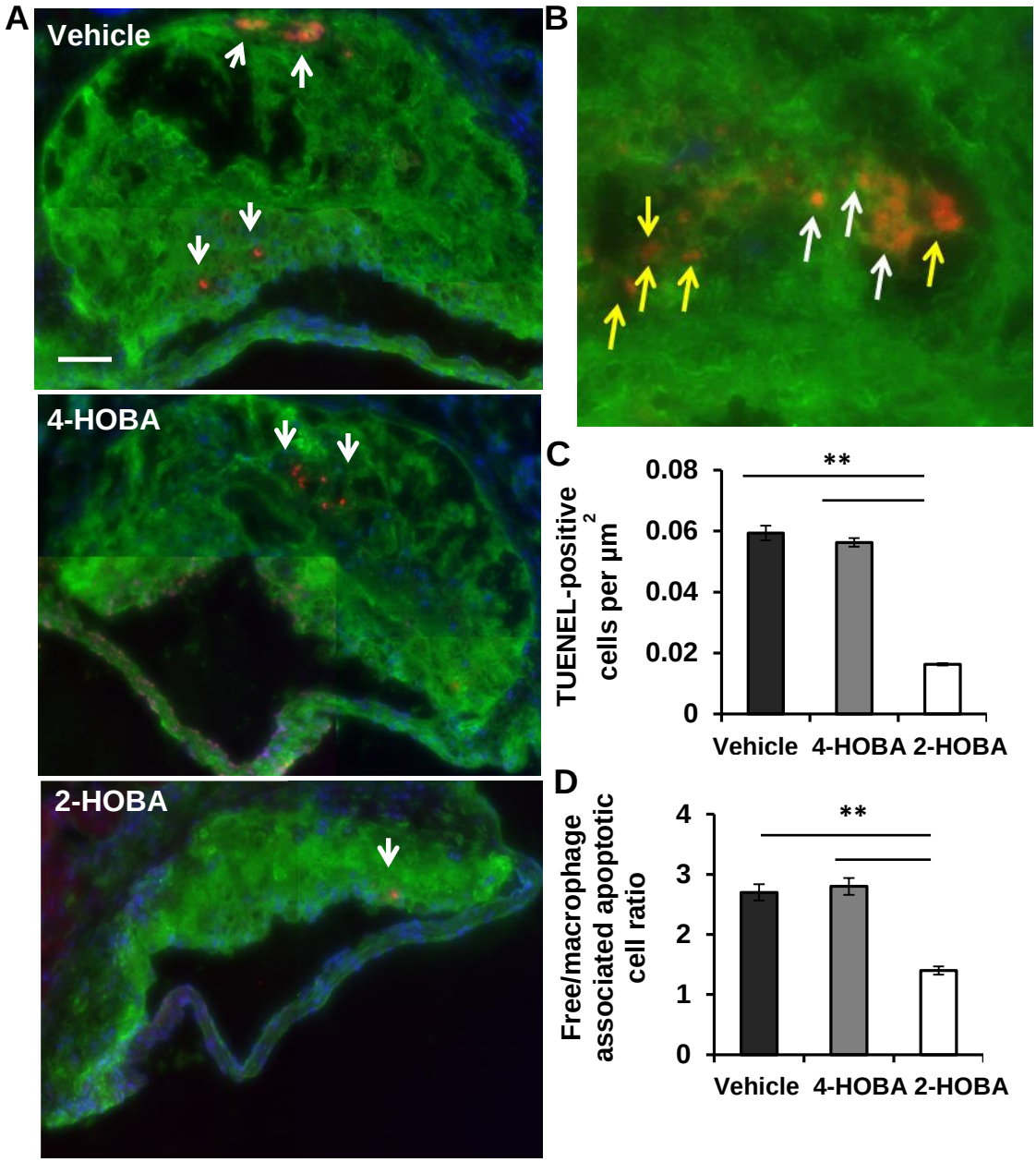

Figure 4. 2-HOBA prevents cell death and increases efferocytosis in atherosclerotic lesions of the *Ldlr*$^{-/-}$ mice. (A) Representative images show dead cells that were detected by TUNEL staining (Red) of proximal aorta sections. Macrophages were detected by anti-macrophage primary antibody (green), and nuclei were counterstained with Hoechst (blue). (B) A representative image taken at a higher magnification to indicate macrophage-associated TUNEL stain (yellow arrows) and white arrows indicate free dead cells that were not associated with macrophages. (C) Quantitation of the number of TUNEL-positive nuclei in proximal aortic sections. (D) Efferocytosis was examined by quantitating the free versus macrophage-

associated TUNEL-positive cells in the proximal aortic sections. Data are presented as mean ± SEM (N = 8 per group). Scale bar = 50 μm, ** $p<0.01$.

Figure 5

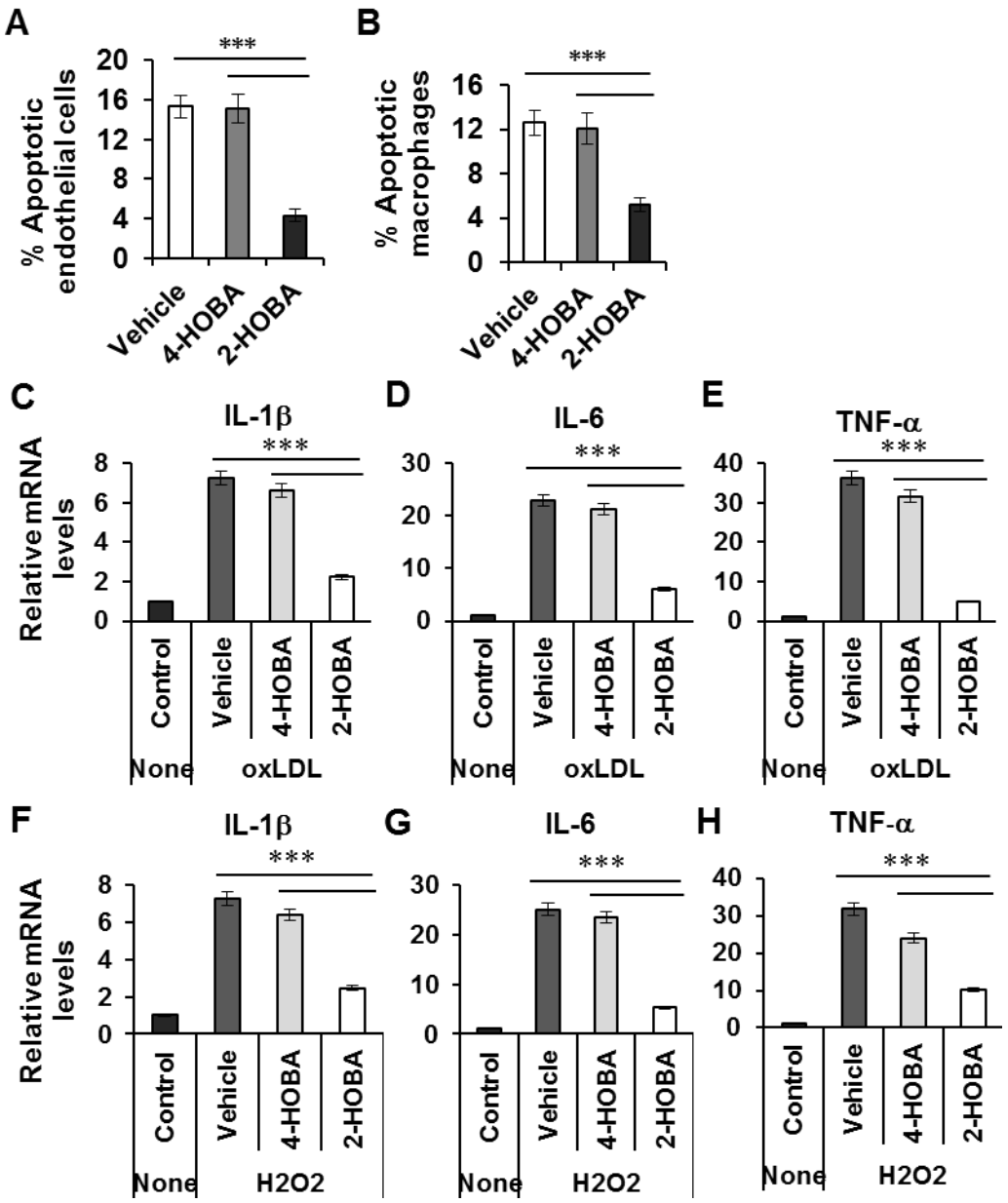

Figure 5. In vitro treatment with 2-hydroxybenzylamine suppresses oxidative stress-induced cell apoptosis and inflammation. (A and B) Mouse aortic endothelial cells (A) or primary macrophages (B) were incubated for 24h with 250 µM H_2O_2 alone or with either 4-HOBA or 2-HOBA. Apoptotic cells were then detected by Annexin V staining and flow cytometry. (C to H) The mRNA levels of IL-1β , IL-6 , and TNF-a were analyzed by real time PCR in the peritoneal macrophages incubated for 24 h with either oxidized LDL (C-E) or 250 µM H_2O_2 (F-H) alone or with either 4-HOBA or 2-HOBA. (A to H) Data are presented as mean ± SEM from three independent experiments, *** $p<0.001$.

Figure 6

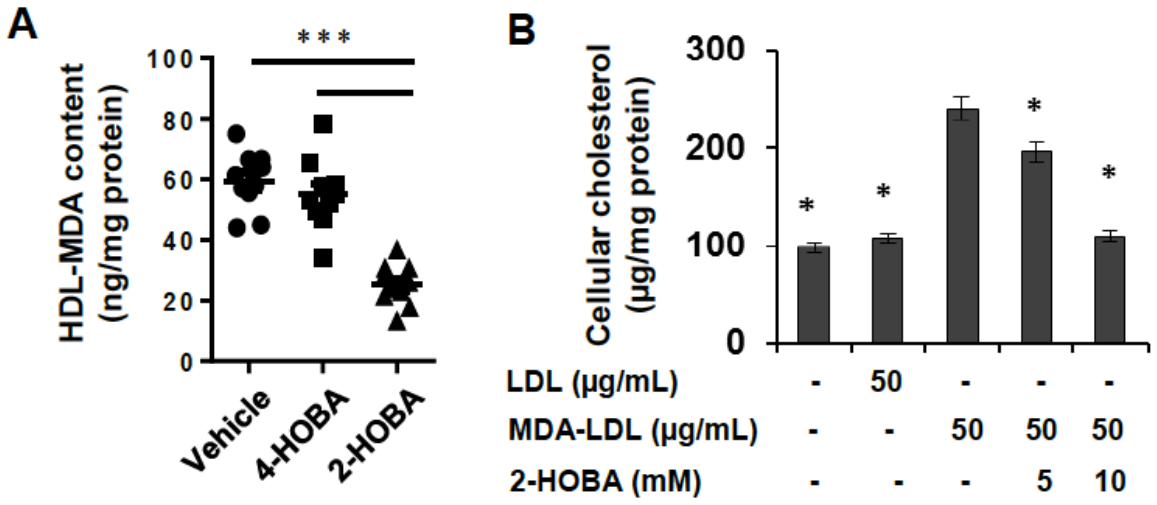

Figure 6. Effects of 2-HOBA on MDA modification of LDL (A) MDA-LDL adducts were measured by ELISA in *Ldlr*$^{-/-}$ mice consuming a western diet for 16 weeks and treated with 2-HOBA, 4-HOBA, or vehicle. N = 10 per group, *** $p<0.001$. (B) LDL was modified in vitro with MDA in the presence of vehicle alone or with 2-HOBA, and then the LDL was incubated for 24h with macrophages and the cellular cholesterol was measured. * $p<0.05$ compared to MDA-LDL alone. Data are representative of 3 independent experiments.

Figure 7

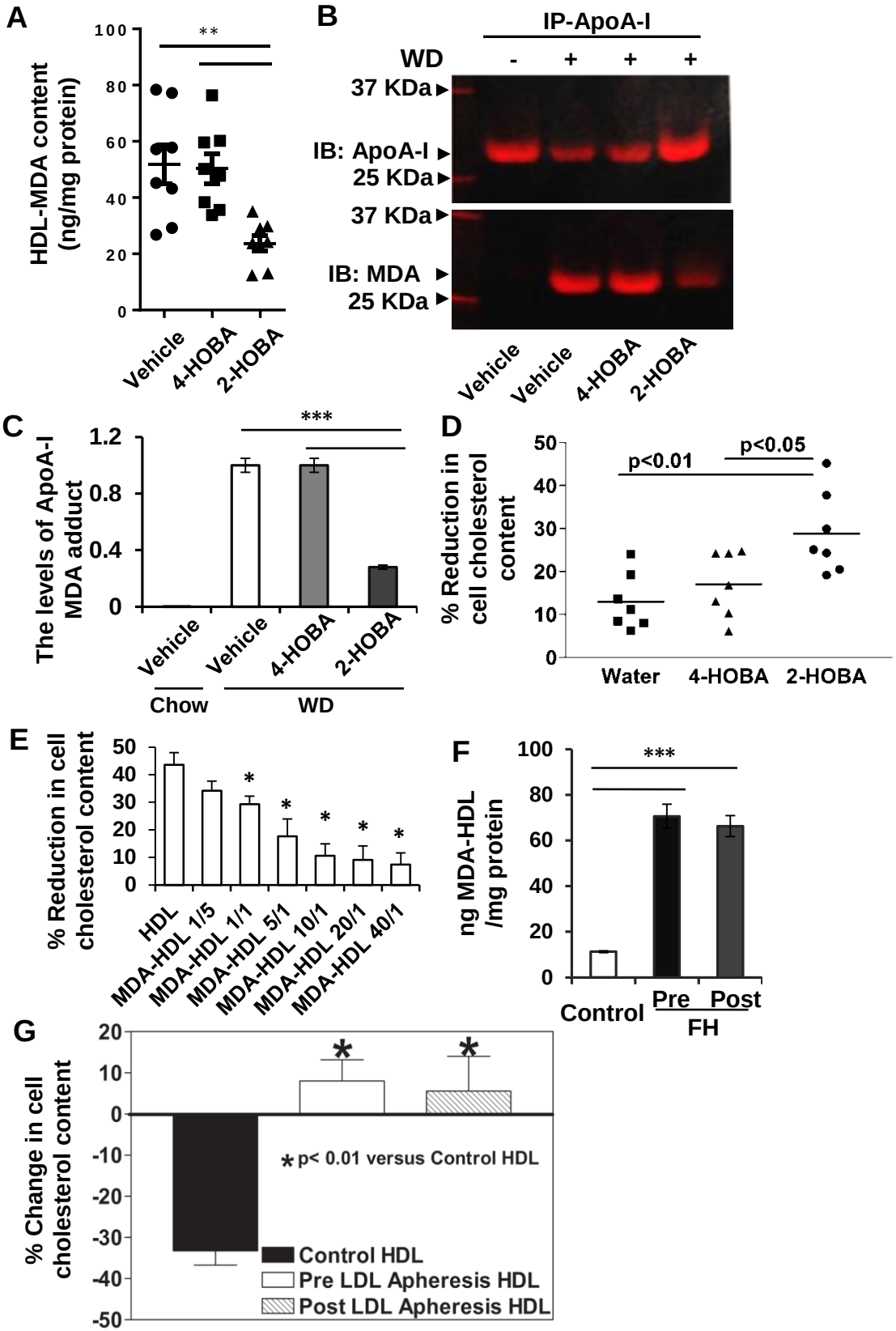
A
HDL-MDA content (ng/mg protein)
100
80
60
40
20
0
**
Vehicle
4-HOBA
2-HOBA
B
IP-ApoA-I
WD
- + + +
37 KDa
IB: ApoA-I
25 KDa
37 KDa
IB: MDA
25 KDa
Vehicle
Vehicle
4-HOBA
2-HOBA
C
The levels of ApoA-I MDA adduct
1.2
0.8
0.4
0
***
Vehicle
Vehicle
4-HOBA
2-HOBA
Chow
WD
D
% Reduction in cell cholesterol content
50
40
30
20
10
0
p<0.01
p<0.05
Water
4-HOBA
2-HOBA
E
% Reduction in cell cholesterol content
50
40
30
20
10
0
*
HDL
MDA-HDL 1/5
MDA-HDL 1/1
MDA-HDL 5/1
MDA-HDL 10/1
MDA-HDL 20/1
MDA-HDL 40/1
F
ng MDA-HDL /mg protein
100
80
60
40
20
0
***
Control
Pre
Post
FH
G
% Change in cell cholesterol content
20
10
0
-10
-20
-30
-40
-50
*
*
* p< 0.01 versus Control HDL
Control HDL
Pre LDL Apheresis HDL
Post LDL Apheresis HDL

Figure 7. Effects of 2-HOBA and HDL-MDA adduct formation on HDL function. (A) The plasma levels of MDA-HDL adducts were measured by ELISA in *Ldlr*$^{-/-}$ mice treated as described in Figure 6. Data are presented as mean ± SEM (N = 8 per group), *** $p<0.001$. (B) Western blots of apoAI and MDA-apoAI in mouse plasma after immunoprecipitation using primary anti-apoAI antibody. *Ldlr*$^{-/-}$ mice were treated as described in Figure 6 and apoAI and MDA-apoAI from plasma of *Ldlr*$^{-/-}$ mice consuming a chow diet are included for comparison. (C) Quantitation using ImageJ software of the mean density (artificial units) of MDA-apoAI detected by Western blotting (B). (D) The HDL was isolated from the plasma of *Ldlr*$^{-/-}$ mice consuming a western diet for 16 weeks and treated with 2-HOBA or 4-HOBA or vehicle. Cholesterol enriched macrophages were incubated for 24h with HDL (25 µg protein/ml), and the % reduction in cellular cholesterol content measured. The levels of HDL-MDA modification was analyzed by ELISA. Data present as mean ± SEM, N = 7 per group, * $p<0.05$, ** $p<0.01$. (E) Human HDL was modified with increasing doses of MDA, and then, the ability of the HDL to reduce the cholesterol content of cholesterol-enriched macrophages was measured. Data are representative of 3 independent experiments. (F) The plasma levels of MDA-HDL adducts were measured by ELISA in control or FH subjects before and after LA. (G) The capacity of HDL from control or FH subjects pre and post LA 9 (n=6 per group) to reduce the cholesterol content of apoE$^{-/-}$ macrophages.